Polymer/Metal Conformal Sliding Contact With Forced Convective Cooling

J. K. Haverstick
Westinghouse Electric Corporation,
4400 Alafaya Trail,
Orlando, FL 32826

T. C. Ovaert
Department of Mechanical Engineering,
The Pennsylvania State University,
University Park, PA 16802

A model for predicting the onset of severe wear for a conformal polymer/metal sliding contact with forced convective cooling has been developed. Finite difference techniques were used for the solution of the bulk contact temperature for the two-dimensional model. The flash temperature was calculated assuming a limiting-case annular, stationary heat source. The limiting load for a given set of operating conditions was solved iteratively, assuming a relationship between strength and temperature, for a heat-resistant polymer, polyethersulphone (PES). An experimental apparatus was constructed, and specimens were tested near the predicted points of wear instability. In addition, specimens were examined using a scanning electron microscope (SEM), and at the most severe operating conditions, signs of thermal softening and gross material transfer were evident. A discussion of model is made in light of the predicted and experimental results.

Introduction

The development of high-strength, heat-resistant polymers has brought about changes in the design and manufacture of many mechanical components. Parts made from polymers are widespread today, including tribological components such as bearings, bushings, and gears. Polymers do have disadvantages, however, in their use as tribomaterials. Perhaps the most significant disadvantage of polymers, particularly thermoplastic based materials, is thermal instability caused by relatively low softening temperatures and low thermal conductivities. The heat generated during sliding can lead to rapid, excessive wear or even seizure of the sliding parts. It is therefore desirable to have predictive models to determine the suitability of a polymeric material for a given sliding configuration.

Most polymers have limits to the proportionality of their specific wear rates when sliding conditions become severe, i.e., at high loads and speeds. The "limiting PV," where P can refer to load or pressure and V to sliding velocity, of a material pair is also frequently tabulated for a specific set of operating conditions and for bearings of a specific size. Uncertainties arise from extrapolation of these limits to other conditions and sizes because of the complicating effects of temperature. It is well known that "limiting PV," also known as severe wear onset or wear instability, is a function of the thermal-dissipative characteristics of the sliding pair in addition to the sliding severity. Thus the same materials may exhibit the onset of severe wear for significantly different pressure-velocity values.

Lancaster (1971) proposed a method for estimating the limiting PV for several thermoplastic polymers and showed good correlation with experimental wear results. The method involves first estimating the total temperature at the sliding interface. If the total temperature is near the softening or melting point of the thermoplastic material then the wear is rapid and can be unstable. Prediction of the sliding interface temperature is therefore the key to predicting the onset of severe wear. In the design of mechanical components, it is essential to ensure that a sliding bearing will operate below the onset of severe wear.

Lancaster used the concept of flash temperatures to predict the onset of severe wear for several thermoplastic materials sliding against steel. In lieu of a tractable flash temperature model like that proposed by Kuhlmann-Wilsdorf (1985, 1987), Lancaster made the assumption of a smooth transition between the two easily derivable cases, namely low speed (steady state) and high speed (fully transient). It was further assumed that the entire load was supported on a single area of contact whose size was determined by the hardness of the softer material in the combination.

Other researchers have performed studies which lend support to the theory of flash temperatures of polymers and predicting the onset of severe wear. Ettles (1987), and Ettles and Shen (1988) proposed that a regime is reached in severe dry sliding of polymers and elastomers in which friction is dominated by heat flow. Ettles coined this "thermal control regime" on the assumption that a maximum attainable temperature is reached in severe sliding. Substituting this maximum attainable temperature into flash temperature equations, the friction coefficient became isolated as a dependent parameter. His results

Contributed by the Tribology Division of The American Society of Mechanical Engineers and presented at the ASME/STLE Tribology Conference, Maui, Hawaii, October 16-19, 1994. Manuscript received by the Tribology Division February 11, 1993; revised manuscript received March 8, 1994. Paper No. 94-Trib-1. Associate Technical Editor: K. Komvopoulos.

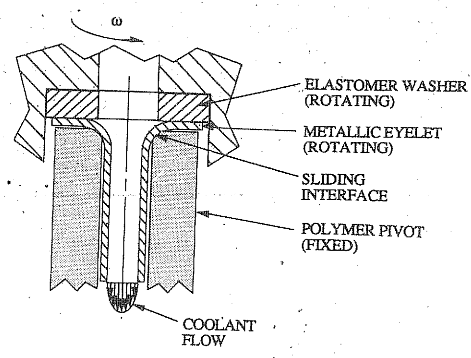

Fig. 1 Two-dimensional polymer-metal sliding contact with forced convective cooling

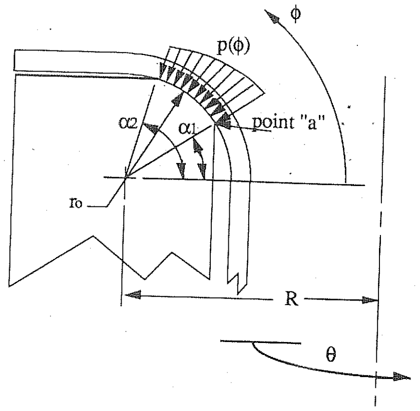

Fig. 2 Pressure distribution

showed good correlation with experimental data for friction coefficients in this regime of sliding.

Theory

Consider a conformal contact as shown in Fig. 1 in which a metallic (stainless steel) eyelet rotates on the inside edge of a cylindrical pivot of a polymeric material (PES). An elastomeric washer above the eyelet distributes a uniform thrust load to the contact. The eyelet and washer rotate together; thus, the sliding interface is between the eyelet and polymeric pivot. A cooling fluid (water) flows axially downward inside the cylindrical body of the eyelet.

In order to predict the limiting operating conditions of the conformal contact described above, the total contact temperature must be estimated. Assuming the ambient temperature is known, the bulk contact temperature is calculated by heat transfer relations requiring a description of the heat input. This description is provided in part by a model of the bulk contact pressure distribution.

Bulk Contact Pressure Distribution. For counterformal contacts, Hertzian pressure distributions are often assumed. However, the conformal contact requires a different approach. One pressure distribution which can be derived analytically is the so-called "uniform wear" model, in which a constant pressure-velocity product across the contact is assumed, as described by Shigley and Mitchell (1983).

As shown in Fig. 2, after initial run-in, the point of contact closest to the centerline, designated as point "a", will have the maximum pressure. The velocity of any point on the surface is proportional to its radius from the centerline. Using the constant "PV" product, the pressure at any point times its radius from the centerline will be equal to the pressure at point "a", designated p_a, times the radius from the centerline to point "a",

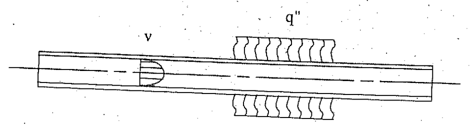

Fig. 3 Thermally developing laminar flow in a duct

$$p(R-r_0\cos\phi)=p_a(R-r_0\cos\alpha_1) \tag{1}$$

Solving for $p(\phi)$,

$$p(\phi)=p_a\frac{(R-r_0\cos\alpha_1)}{(R-r_0\cos\phi)}. \tag{2}$$

A differential element of the vertically applied load, dP, is equal to the pressure times the differential area projected vertically,

$$dP=p(\phi)dA\sin\phi \tag{3}$$

where the differential surface area element of a torus, dA, can be expressed as:

$$dA=r_0\,d\phi(R-r_0\cos\phi)d\theta. \tag{4}$$

Substituting Eqs. (2) and (4) into (3) and integrating gives an expression for the vertically applied load, P,

$$P=2\pi r_0p_a(R-r_0\cos\alpha_1)(\cos\alpha_1-\cos\alpha_2). \tag{5}$$

Solving for the maximum pressure, p_a, and substituting into Eq. (2) provides the pressure distribution

$$p(\phi)=\frac{P}{2\pi r_0(R-r_0\cos\phi)(\cos\alpha_1-\cos\alpha_2)}\ \{\alpha_1\le\phi\le\alpha_2\}. \tag{6}$$

Equation (6) shows that the pressure distribution is a function of the contact angles, α_1 and α_2, and varies with the coordinate, ϕ.

The differential friction torque, dQ, can be expressed as the friction coefficient, μ, multiplied by the pressure, p, the differential area element, dA, and the torque arm, r, which is the distance from the centerline to the differential area element.

$$dQ=\mu rpdA \tag{7}$$

The torque arm, r, can be written as

$$r=R-r_0\cos\phi. \tag{8}$$

Substituting Eqs. (3), (8), and (6) into Eq. (7) and integrating this over the contact area gives the following expression for the friction torque:

$$Q=\frac{\mu P}{(\cos\alpha_1-\cos\alpha_2)}[R(\alpha_2-\alpha_1)+r_0(\sin\alpha_1-\sin\alpha_2)] \tag{9}$$

For a given polymer pivot, α_1 is assumed to remain constant for the duration of the life of the bearing, while α_2 increases with the wear of the polymer pivot. From Eq. (9), as the bearing wears, the friction torque, Q, will decrease as α_2 approaches 90 deg.

Convective Heat Transfer. Next, consider a model of internal laminar flow through a duct as shown in Fig. 3. One may further assume that the fluid has a uniform temperature and the velocity profile of the fluid is fully developed upstream of the uniform heat flux, q''. When the fluid reaches the uniform heat flux, a development length is required before the temperature profile becomes established. This distance is referred to as the thermal entry length.

Shah and London (1978) list expressions for the Nusselt number, Nu, for the above conditions. For the mean Nusselt number,

$$\mathrm{Nu}_m=\begin{Bmatrix}1.953\,(x^*)^{-1/3} & \text{for } x^*\le 0.03\\ 4.364+\dfrac{0.0722}{x^*} & \text{for } x^*>0.03\end{Bmatrix} \tag{10}$$

and the local Nusselt number,

$$\frac{Nu_x+1}{5.364}=\left[1+\left(\frac{220}{\pi}x^*\right)^{-10/9}\right]^{3/10} \tag{11}$$

The dimensionless coordinate, x^*, is defined as

$$x^*=\frac{x/D}{\mathrm{Re\ Pr}} \tag{12}$$

where D is the duct diameter, Re is the axial Reynolds number, and Pr the Prandtl number. These expressions are curve fits to an analytical solution of the laminar flow problem.

In this model, the convective heat transfer is a function of the volumetric flow rate and the coordinate distance from the entrance, whereas convection for flow with fully developed velocity and temperature profiles is independent of the volumetric flow and the axial coordinate.

Investigation of the effects of rotation on heat transfer of laminar flow in axially rotating ducts reveals an interesting find and some deficiencies. McElhiney and Preckshot (1977) performed an experimental study for the case of a uniform velocity and temperature profile at the entrance of a horizontally rotating tube with a constant wall temperature. Their experiments typically showed an enhancement in heat transfer over that in a non-rotating duct on the order of 15 to 20 percent up to a critical rotational speed. Above a critical speed, severe deterioration of the heat transfer was observed. The degradation of the cooling was believed to be caused by the formation of a stagnant layer of fluid in the entrance of the rotating duct.

It is difficult to apply the results from this study because of the difference in velocity profile assumption (uniform versus fully developed), boundary condition (constant wall temperature versus constant heat flux), and tube orientation (horizontal versus vertical). However, it is not unreasonable to assume an enhancement of 15 percent due to axial rotation, provided that the swirl ratio is below the critical level. The following relationship was given for the critical swirl ratio:

$$\mathrm{Re}_A\Gamma^{0.9381}=7757 \tag{13}$$

where Γ, the swirl ratio, is defined as

$$\Gamma=\frac{\mathrm{Re}_R}{\mathrm{Re}_A}. \tag{14}$$

The axial Reynolds number, Re_A, is

$$\mathrm{Re}_A=\frac{Dv}{\nu} \tag{15}$$

and the rotational Reynolds number, Re_R, is

$$\mathrm{Re}_R=\frac{D^2\omega}{\nu} \tag{16}$$

where v is the average axial fluid velocity, ω is the rotational speed, and ν is the kinematic viscosity.

Conduction Heat Transfer. The axis of symmetry coincident with the axis of rotation may be used to simplify the problem from three-dimensional to two-dimensional conduction. The differential equation for heat conduction with no internal heat generation is:

$$\nabla^2T=\frac{\rho c}{k}\frac{\partial T}{\partial t}. \tag{17}$$

Due to the curvature in the vicinity of the contact, different coordinate systems should be used for the differential equations. Figure 4 shows three coordinate system zones. Zone 1 requires a cylindrical coordinate system, zone 2 a toroidal coordinate system, and zone 3 a cylindrical coordinate system. The differential equations for two-dimensional heat conduction are:

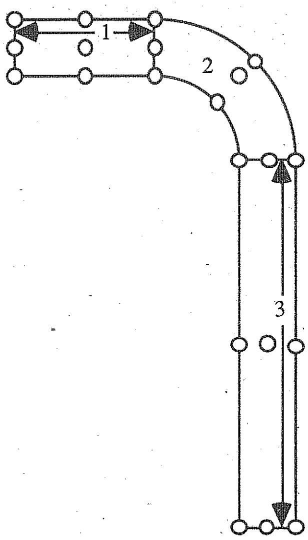

Fig. 4 Part geometry and zones for finite difference solution

Cylindrical (zones 1 and 3):

$$\frac{\partial^2T}{\partial r^2}+\frac{1}{r}\frac{\partial T}{\partial r}+\frac{\partial^2T}{\partial z^2}=\frac{\rho c}{k}\frac{\partial T}{\partial t} \tag{18}$$

Toroidal (zone 2):

$$\frac{\partial^2T}{\partial r_1\partial r_2}+\frac{1}{r_1}\frac{\partial T}{\partial r_2}+\frac{1}{r_2}\frac{\partial T}{\partial r_1}+\frac{\cos\alpha}{r_1r_2\sin\alpha}\frac{\partial T}{\partial\alpha}+\frac{1}{r_1r_2}\frac{\partial^2T}{\partial\alpha^2}=\frac{\rho c}{k}\frac{\partial T}{\partial t}. \tag{19}$$

Since the metal will typically be several orders of magnitude more thermally conductive than the polymer, the heat evolved at the sliding contact will be conducted entirely by the metal, except for a negligibly small amount conducted by the polymer or elastomer surfaces. Therefore, polymer or elastomer boundaries are assumed to be adiabatic, with the exception of the contact region. In the contact region the boundary condition is a specified heat flux, equal to the product of the friction coefficient, the bulk contact pressure, and the sliding velocity.

Recalling that the pressure-velocity product was assumed uniform across the contact, the heat flux in the contact region will also be uniform, provided that the friction coefficient is constant as well. from Eq. (6), the heat flux is then:

$$q''=\frac{\mu P\omega}{2\pi r_0(\cos\alpha_1-\cos\alpha_2)}. \tag{20}$$

Internal surfaces which contact the cooling fluid require a convection boundary condition. The convection coefficient, h, can be found from the expressions for Nusselt number. In external flow convection problems, a constant ambient temperature is usually assumed. However, for heat transfer by internal flow in a duct, the bulk fluid temperature is usually not constant over the length of the duct. In this problem, the bulk fluid temperature is coupled with the convection heat transfer.

The conduction problem is now fairly complex and requires numerical techniques for solution. Using finite difference methods, the differential equations can be solved with the boundary conditions discussed above. Using data from transient finite difference solutions, the steady-state temperature distribution of the fluid in the tube can be approximated. This decouples the problem and enables an iterative solution by successive over-relaxation.

The total rise in temperature of the cooling fluid for a given set of operating conditions can be predicted using an energy balance. Since all the heat evolved at the sliding contact is convected by the internal fluid flow, the temperature rise can be expressed as:

Table 1 Geometry and material properties

Geometry		
R		1.21 mm
r_0		0.33 mm
L		6.31 mm
R_f		1.34 mm
R_f'		1.55 mm
w		0.127 mm
Properties for stainless steel		
Mass density	ρ	8018 kg/m³
Specific heat	c	0.502 J/kg K
Thermal conductivity	k	16.26 W/m K
Properties for saturated water at 104°F		
Mass density	ρ	994.59 kg/m³
Specific heat	c	4.1784 J/kg K
Thermal conductivity	k	0.628 W/m K
Kinematic viscosity	ν	0.658 m²/s
Prandtl number	Pr	4.34

$$\Delta T_b = \frac{Q\omega}{\rho c \dfrac{dV}{dt}} \tag{21}$$

where Q is the torque calculated from Eq. (9), and dV/dt, ρ, and c are the volumetric flow rate, the mass density, and the specific heat, respectively, of the fluid.

For the configuration shown in Fig. 4, and the geometric variables and material properties defined in Table 1, the maximum bulk contact temperature can be found.

Flash Temperatures. For the case of plastic contacts, the size of a contact spot is determined by the hardness or flow pressure of the softer material in the combination, rather than by the respective elastic constants. The contact spot radius therefore is:

$$R = \sqrt{\frac{P}{H_s \pi N}} \tag{22}$$

where P is the applied load, H_s is the flow pressure of the softer material (polymer), and N is the number of contact spots.

The size of the contact spots, or the real area of contact, is a function of load since the spots are assumed to be plastic. If a vertically applied load is reacted on an inclined angle, as in the case for an angular contact thrust bearing, the force normal to the contact surface is greater than the vertically applied load. Therefore an effective load, which is normal to the contact surface, determines the size of the contact spot. For a contact as in Fig. 1, where the contact angle is variable, a suitable average contact angle is needed to calculate an effective load. The value of the bulk pressure distribution is equal to the average contact pressure when the coordinate ϕ is equal to α_{avg}, defined as:

$$\cos \alpha_{avg} = \frac{\cos \alpha_1 + \cos \alpha_2}{2}. \tag{23}$$

Therefore the effective load for an angular conformal contact can be approximated as:

$$P_{eff} = \frac{P}{\sin \alpha_{avg}}. \tag{24}$$

Lancaster (1971) showed that for several thermoplastic materials, the indentation hardness of many thermoplastic polymers decreased nearly exponentially with increasing temperature. Hardness was expressed as:

$$H_s = H_{s,0} e^{-\alpha(T-T_0)} \tag{25}$$

where $H_{s,0}$ was the hardness at T_0, room temperature, and α was a material constant. Lancaster found that the values of the material constant, α, did not differ greatly between the various polymers tested and suggested a value for α of 0.005 as typical.

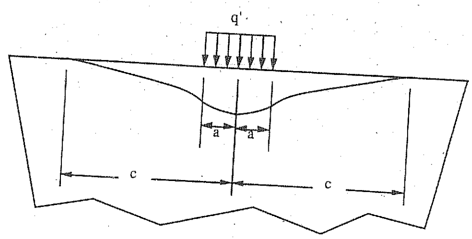

Fig. 5 Stationary band source of heat applied to a semi-infinite body

Tanaka and Yamada (1985) investigated the friction and wear properties of several of the newer heat-resistant polymers, including PES. These investigators found that PES did not follow Lancaster's hardness-temperature relationship since the hardness was nearly constant up to 150°C. Though Tanaka and Yamada did not present any hardness data for PES above this temperature, it is probable that the hardness of PES drops off rather sharply near the softening point, in which case an assumption of constant hardness up to the softening temperature is reasonable and used in this model.

Stationary Heat Source—A Limiting Case. For a polymer/metal conformal contact, the assumption of a single, circular contact spot may not be the best choice. The radius of a single, circular, plastic contact spot in this case is on the same order of magnitude as the bearing dimensions. It is more likely that the contact spots for a run-in bearing would be long in the sliding direction and thin in the direction perpendicular to sliding, as discussed by Ovaert and Cheng (1991).

In a conformal contact, a limiting case for the shape of the contact region would simply be annular. For an annular contact spot sliding on itself, the heat source would now be stationary and fully steady-state. Since no heat can be conducted in the direction of sliding, the problem becomes two-dimensional rather than three-dimensional. Figure 5 illustrates a stationary band source of heat applied over a half-space, assuming that the contact spot is plastic. The maximum temperature due to a stationary band source of heat, q', can be found from Johnson (1985).

$$\Delta T_{flash,lim} = \frac{2q'}{\pi k_2}\left[(a+c)\ln\left(\frac{a+c}{a}\right)^2 + (a-c)\ln\left(\frac{a-c}{a}\right)^2 \right] \tag{26}$$

where a is the half-width of the band source and c is arbitrarily chosen as the half-width of the bulk contact as shown in Fig. 5.

Strength-Temperature Relationship. Lancaster (1971) mentioned the importance of a strength-temperature relationship in estimating the limiting PV for onset of severe wear in polymers. Since a bearing can support low stresses at temperatures close to the melting point, the limiting temperature at high stresses will be lower than the melting point. If a variation of strength with temperature is assumed, it would then be possible to determine the limiting temperature corresponding to any given level of stress.

Using elevated-temperature tensile strength data points for PES and assuming that the material fails by a shear mode, as most ductile materials do, then the corresponding shear strengths can be found. These points can be fit to a curve of the form $T_{lim} = T_0 - a\tau^b$, where T_{lim} represents limiting temperature, τ represents shear strength, and T_0, a, and b are constants. The resulting curve fit to the data points is

$$T_{lim}(°C) = 203 - (3.663 \times 10^{-3})\tau^{2.896} \tag{27}$$

Table 2 Elevated-temperature strength data for PES

Tensile strength (MPa)	Temperature (°C)	Shear strength (MPa)
84	20	42
55	150	27.5
41	180	20.5
0	203	0

where τ is in units of MPa. The strength data points for PES from the manufacturer (ICI Advanced Materials) are shown in Table 2. The data points and curve fit are plotted in Fig. 6.

Limiting Load Versus Flow Rate. For each loading condition (thrust load, coefficient of friction, and contact angles) there is a corresponding state of stress at the average contact angle, α_{avg}, on the polymer pivot. In addition to the average bulk contact pressure acting in compression, a shear traction due to friction at the surface is present. Additionally, because the thrust load is reacted by an angular contact, a tangential tensile (hoop) stress component exists at the average contact angle. The maximum shear stress for the given stress state can be found from Mohr's circle transformation equations.

For this maximum shear stress, a corresponding limiting temperature, T_{lim}, exists which can be found from the curve fit of elevated temperature points. This is the theoretical maximum temperature at which the material could support the shear stress without failing.

The total operating temperature, T_{oper}, for a given set of operating conditions is found from the sum of the three temperature components: ambient temperature, bulk contact temperature, and flash temperature. The bulk contact temperature is found from the 2-D finite difference model, and the flash temperature is calculated assuming the limiting case of an annular, stationary heat source.

From a given set of operating conditions, it is now possible to estimate whether the wear will be severe. The difference, ϵ, between the limiting temperature and the operating temperature shall be the criterion for severe wear onset.

$$T_{lim} - T_{oper} = \epsilon \tag{28}$$

If ϵ is negative or zero, then severe wear should occur. If ϵ is positive, then the wear should be stable. If all operating conditions except the thrust load, P, are held constant, Eq. (28) can be solved iteratively for $\epsilon = 0$. This would give a limiting load for a set of operating conditions.

Figure 7 shows a plot of limiting load versus coolant flow rate for friction coefficients of 0.1, 0.25, and 0.4. The friction coefficient affects the limiting load in two ways. First, friction determines the heat loading for both bulk contact temperature and flash temperature. The friction coefficient also enters into the equation for the maximum shear stress for the stress state. The plot shows that the coolant flow plays a significant role only at very low coolant flow rates. At these low flows, the heat evolved at the sliding interface is not dissipated as effectively.

Experimental

A test apparatus was constructed for the primary purpose of characterizing the operation of the bearing configuration. The test apparatus is illustrated in Fig. 8. A normal load is applied from above the rotating contact while the rotation is driven by an vibration-isolated variable speed motor with an elastomer o-ring belt drive. Water from a temperature-controlled bath was pumped through the rotating contact by a peristaltic pump at very low flow rates (ml/min.). A reaction torque transducer below the contact was used to measure the very small frictional torques produced by the rotating contact.

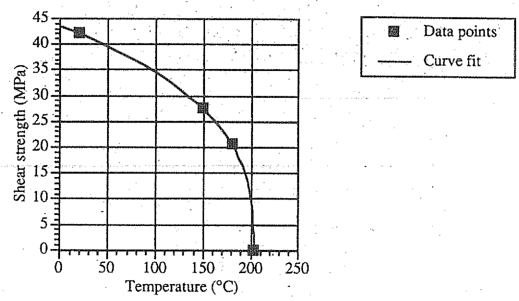

Fig. 6 Strength-temperature relationship for PES

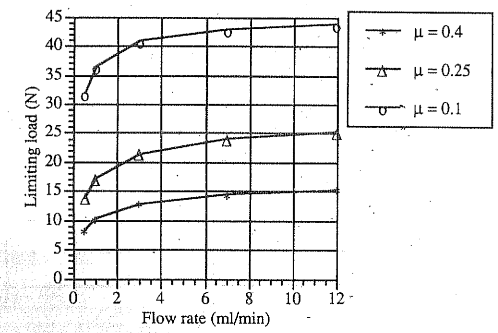

Fig. 7 Limiting load versus flow rate. Speed = 3600 rpm, α_1 = 33 deg, α_2 = 90 deg.

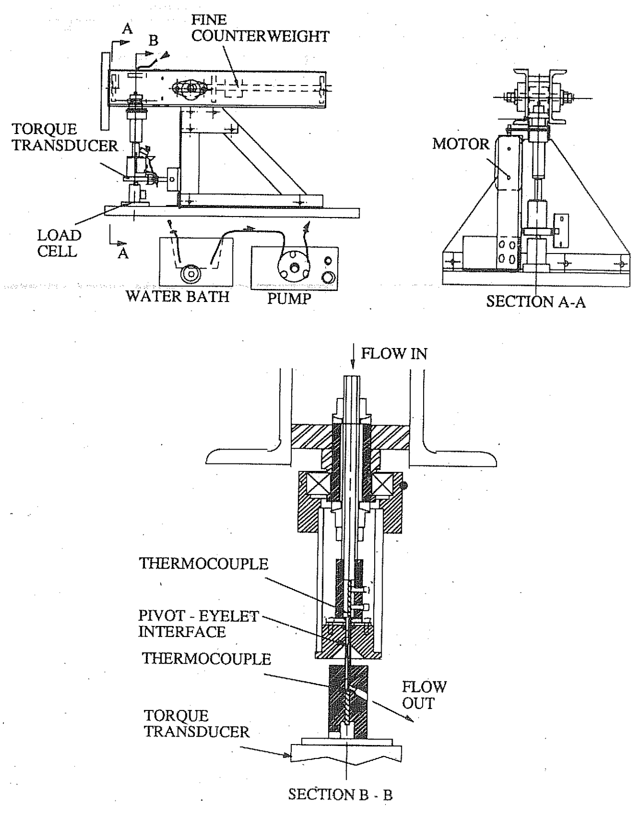

Fig. 8 Test apparatus

The load cell was used to measure the applied normal load. Hyperdermic thermocouples (0.25 mm diameter) were placed directly above and below the contact to measure the temperature of the water before and after passing through the bearing region. The two thermocouples, the torque transducer, and the load cell were interfaced with a data acquisition system linked to a personal computer to enable recording and proc-

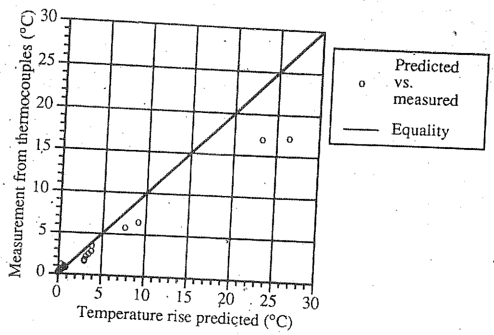

Fig. 9 Measured versus predicted fluid temperature rise

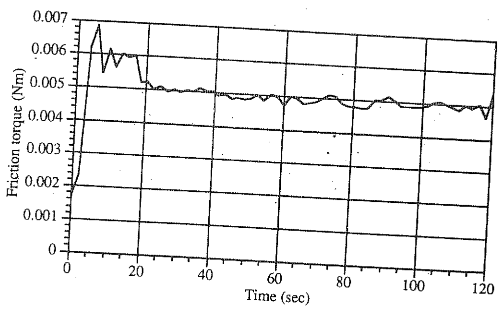

Fig. 10 Reaction torque versus time. Conditions: nominal load = 13.3 N, speed = 3600 rpm, coolant flow rate = 7 ml/min.

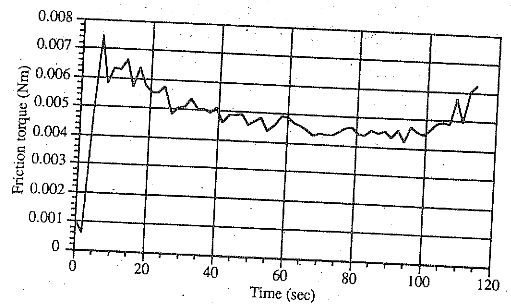

Fig. 11 Reaction torque versus time. Conditions: nominal load = 13.3 N, speed = 3600 rpm, coolant flow rate = 1 ml/min.

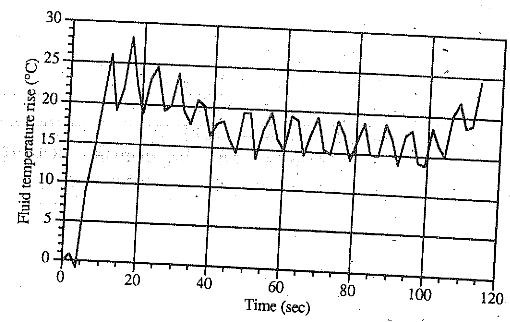

Fig. 12 Fluid temperature rise versus time. Conditions: nominal load = 13.3 N, speed = 3600 rpm, coolant flow rate = 1 ml/min.

essing of data. In the experiments, wear rates were not measured, since they were expected to be very small for most cases. Due to the small size and the rapid rotational speed of the eyelet, it was not possible to measure the bulk contact temperature. The apparatus monitored friction behavior versus time for various loads, speeds, and coolant flow rates. The water temperature data could be used to help correlate the operating characteristics with the analytical model. Water flow rates were varied from 12 ml/min. to 1 ml/min.

Test Data Description. The raw data points were filtered to show trends more readily. For most of the specimens, reaction torque due to friction was steady over the test duration. Unlubricated PES specimens typically had dynamic friction coefficients of 0.3 to 0.4. Tanaka and Yamada (1985) reported friction coefficients ranging from 0.3 to 0.6 for unlubricated PES on stainless steel in a pin-on-disk configuration, with steady-state friction coefficients ranging from 0.5 to 0.55.

The reaction torque is a very important quantity to measure since the product of reaction torque and rotational speed is equal to the rate at which energy is evolved into heat during sliding. Figure 9 shows the experimental correlation between the predicted and measured fluid temperature rise at 3600 rpm for various water flow rates. The predicted fluid temperature rise is a function of friction torque, speed, and flow rate, as expressed in Eq. (21).

The apparatus was run at higher loads in an attempt to investigate severe wear failures. Tests were conducted at loads as high as 13.3 N in attempts to produce severe wear onset. Due to structural limitations of the torque transducer, no thrust loads higher than 13.3 N were used. These tests were performed at various coolant flow rates for comparison with the theoretical predictions shown in Fig. 7. Reaction torque results are shown in Fig. 10 for a test with a nominal thrust load of 13.3 N, rotational speed of 3600 rpm, and a coolant flow rate of 7 ml/min. After initial run-in, the reaction torque is relatively steady at 0.005 N-m, which corresponds to a friction coefficient of approximately 0.3. The fluid temperature rise across the bearing correlates with the torque data. From Fig. 7, these operating conditions are not expected to produce severe wear, which correlates with the experimental data since the friction levels off. Figures 11 and 12 show reaction torque and temperature data, respectively, for a test performed at the same conditions, except for a coolant flow rate of 1 ml/min. After run-in of the contact, the friction shows a definite increase toward instability before the data terminates. From Fig. 7, these operating conditions are close to those predicted to cause severe wear.

Discussion

The polymer pivot and stainless steel eyelet specimens discussed above were examined using a scanning electron microscope (SEM). Comparing Figs. 13(*a*) and 14(*a*) for the worn PES pivot surfaces, Fig. 14(*a*) (1 ml/min. flow rate) revealed an overall smoother appearance than Fig. 13(*a*) (7 ml/min. flow rate). Though not universally true, in this case for PES the smoother worn surface corresponds to a greater degree of thermal softening, particularly for this annular conformal contact. Comparing Figs. 13(*b*) and 14(*b*), one can see the significantly greater amounts of gross PES transfer to the eyelet surface at the 1 ml/min. flow rate, also indicative of a high degree of thermal softening. Although the micrographs show signs of thermal softening with the predominantly low coolant flow rates, the wear in both cases was stable since the PES pivot was not worn to the point where the flange of the eyelet was in sliding contact with the top surface of the polymer pivot (Fig. 1). This suggests that the predictive model for severe wear onset described above is somewhat conservative.

One potential reason that severe wear did not occur as expected is that the model predicts fluid/surface temperatures above the boiling point of water for the expected failures at a load of 13.3 N. The presence of two-phase flow means a significant enhancement in convective cooling which was not accounted for in the model. The cooling enhancement translates into lower contact temperatures than predicted, resulting in higher limiting loads.

The predicted temperatures were higher than the measured temperatures particularly at the lower flow rates: The error is believed to be caused by the flow characteristics of the per-

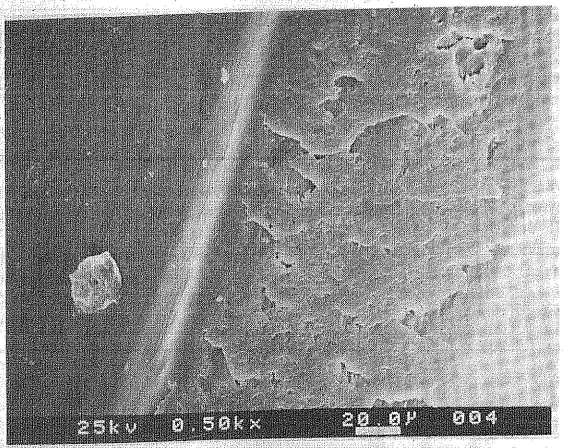

Fig. 13(*a*) Worn PES pivot surface. Conditions: nominal load = 13.3 N, speed = 3600 rpm, coolant flow rate = 7 ml/min. Magnification 500 ×.

Counterface sliding direction ↑

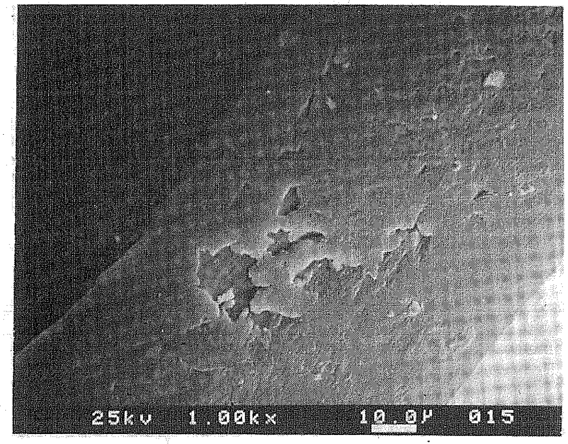

Fig. 14(*a*) Worn PES pivot surface. Conditions: nominal load = 13.3 N, speed = 3600 rpm, coolant flow rate = 1 ml/min, magnification 1000 ×.

Counterface sliding direction ↑

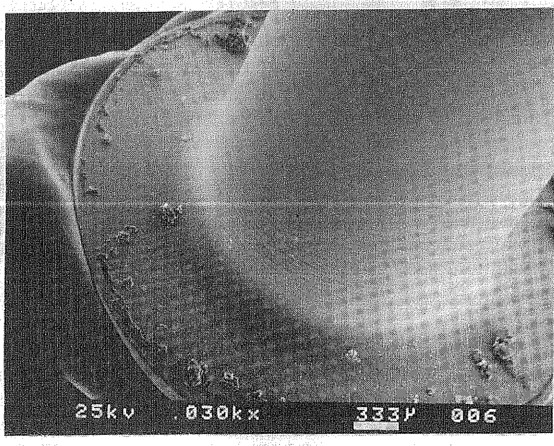

Fig. 13(*b*) Worn eyelet surface. Conditions: nominal load = 13.3 N, speed = 3600 rpm, coolant flow rate = 7 ml/min, magnification 30 ×.

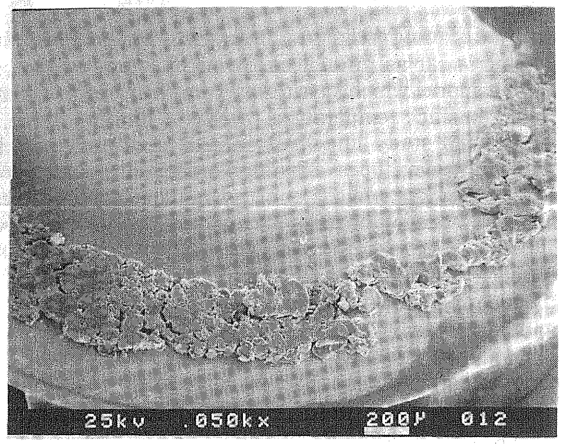

Fig. 14(*b*) Worn eyelet surface. Conditions: nominal load = 13.3 N, speed = 3600 rpm, coolant flow rate = 1 ml/min, magnification 50 ×.

istaltic pump. The pump flow is periodic, rather than constant and actually pulls back a small amount of flow at each cycle. This "draw back" phenomenon can cause heated fluid to pass back over the upstream thermocouple, thereby producing a net lower fluid temperature rise measurement and the periodic temperature data as seen in Fig. 12.

The assumption of a single, annular contact spot and hence a fully steady-state, stationary heat source was a worst-case for calculating flash temperatures. It is reasonable to assume that a more realistic flash temperature estimate would fall somewhere between that calculated for the stationary source mentioned above and that for a moving heat source (fully transient). This, in turn, would also allow for higher limiting loads.

As mentioned previously, structural limitations of the torque transducer precluded any testing with loads larger than 13.3 N. A test apparatus capable of generating higher loads would have been more effective for producing more results showing severe wear; however a trade-off had to be made to obtain the desired torque measurement sensitivity at the expense of load capacity. In addition, redesign of the test apparatus incorporating a "passive" load/torque sensor arrangement is expected to further alleviate this issue.

Conclusions

1. A model for predicting the onset of severe wear was created for a conformal polymer/metal sliding contact with forced convective cooling.

2. The predicted temperatures were slightly higher than the measured temperatures particularly at the lower flow rates. The error is believed to be caused by the flow characteristics of the peristaltic pump and fluid delivery system. Overall, the model showed reasonably good agreement with the experimental data.

3. All wear on the specimens was stable, as determined from the microscopic examinations; however, at the most severe operating conditions, some signs of thermal softening were evident. In general, the model underestimated limiting loads and was therefore conservative. It is believed that the predicted severe wear failures were not observed due to the presence of two-phase flow in the cooling fluid and due to the use of a limiting case to predict the flash temperatures at the contact. Convective cooling is enhanced significantly for two-phase flow, causing lower bulk contact temperatures and therefore higher limiting loads. In addition, a more realistic estimate of the flash temperature would be somewhat between that of a stationary heat source (limiting case) and a moving heat source, which would also allow for higher limiting loads.

Acknowledgments

The authors gratefully acknowledge the generous support from Baxter Healthcare Corporation, Fenwal Division. Special thanks go to Dr. Donald Schoendorfer for his help throughout the investigation.

References

Ettles, C. M. M., 1987, "Polymer and Elastomer Friction in the Thermal Control Regime," *ASLE Transactions*, Vol. 30, pp. 149–159.

Ettles, C. M. M., and Shen, J. H., 1988, "The Influence of Frictional Heating on the Sliding Friction of Elastomers and Polymers," *Rubber Chemistry and Technology*, Vol. 61, pp. 119–136.

ICI Advanced Materials, "Victrex PES Properties and Introduction to Processing," ICI Advanced Materials Business Group, Welwyn Garden City, England.

Johnson, K. L., 1985, *Contact Mechanics*, Cambridge University Press, Cambridge, pp. 374–396.

Kuhlmann-Wilsdorf, D., 1985, "Flash Temperatures Due to Friction and Joule Heat at Asperity Contacts," *Wear*, Vol. 105, pp. 187–198.

Kuhlmann-Wilsdorf, D., 1987, "Temperatures at Interfacial Contact Spots: Dependence on Velocity and on Role Reversal of Two Materials in Sliding Contact," ASME JOURNAL OF TRIBOLOGY, Vol. 109, pp. 321–329.

Lancaster, J. K., 1971, "Estimation of the Limiting PV Relationships for Thermoplastic Bearing Materials," *Tribology*, Vol. 4, pp. 82–86.

McEhiney, J. E., and Preckshot, G. W., 1977, "Heat Transfer in the Entrance Length of a Horizontal Rotating Tube," *International Journal of Heat and Mass Transfer*, Vol. 20, pp. 847–854.

Ovaert, T. C., and Cheng, H. S., 1991, "The Unlubricated Sliding Wear Behavior of Polyetheretherketone against Smooth Mild-Steel Counterfaces," ASME JOURNAL OF TRIBOLOGY, Vol. 113, No. 1, pp. 150–157.

Tanaka, K., and Yamada, Y., 1985, "Effect of Temperature on the Friction and Wear of Some Heat-Resistant Polymers," *Polymer Wear and Its Control*, L. H. Lee, ed., American Chemical Society, Washington, DC, pp. 103–128.

Shah, R. K., and London, S. L., 1978, *Laminar Flow Forced Convection in Ducts*, Academic Press, New York.

Shigley, J. E., and Mitchell, L. D., 1983, *Mechanical Engineering Design*, McGraw-Hill, New York, NY.

DISCUSSION

F. E. Kennedy, Jr.[1]

I enjoyed reading this paper. It presents the results of a study of polymer wear as influenced by surface temperature, and develops a model which says that severe wear begins when the polymer's surface temperature reaches a limiting value. We have a related study underway in our laboratory and have independently developed a similar model, although for different polymer materials (Kennedy and Tian, 1993). Because of my interest in their model and results, I wish to direct several clarifying questions to the authors.

The authors' model is based on a limiting temperature (Eq. (27)) which includes a temperature-dependent shear strength. It is not clear how Eq. (27) is used, though, since temperature is included on both sides of the equation, albeit implicitly in the shear strength term on the right-hand side. In the discussion surrounding Eq. (28) it appears that a temperature is first determined for a given set of operating conditions and it is used to find whether the limiting load has been exceeded. However, as is stated by the authors, both surface temperature and shear stress are a function of friction coefficient, which may also be a function of temperature, as the authors' experiments show. How can the model be used in predicting wear failure if neither the surface temperature nor the friction coefficient is known a-priori?

The authors' experimental results include several quantities that aren't quite clear. I hope they can clarify the following points in their Closure:

What is the relationship between frictional torque (Figs. 10 and 11) and friction coefficient? How much variation of friction coefficient occurred in the tests?

The measured friction coefficient seemed to be in the range of 0.3 and this is a bit lower than the unlubricated friction coefficients quoted for the PES material. Was any of the cooling water present at the contact interface to cause a reduction of friction? Was any leakage of water noted through the PES/stainless steel contact interface?

The authors state that some tests were conducted at operating conditions close to those predicted to cause severe wear. Our tests have shown that polymer wear rates increase drastically once the limiting surface temperature is reached. Have the authors been able to note such transitions to severe wear, perhaps in tests with a different torque sensor? Will any attempt be made to measure wear rates in future tests so that the transition to severe wear can be well characterized?

[1]Thayer School of Engineering, Dartmouth College, Hanover, NH 03755.

Additional Reference

Kennedy, F. E., and Tian, X., 1993, "The Effect of Interfacial Temperature on Friction and Wear of Thermoplastics in the Thermal Control Regime," presented at *20th Leeds-Lyon Symposium on Tribology*, Lyon, France. To be published in *Dissipative Processes in Tribology*, D. Dowson, et al., eds.

Authors' Closure

The authors would like to thank Professor Kennedy for his comments and questions on our work. First of all, friction coefficient must be input into this model. This is due to the fact that prediction of the friction coefficient is unlikely and much more difficult than the other variables for this configuration.

Friction coefficient is related to friction torque by Eq. (9), which is derived from the contact geometry. Due to the very small size and geometry of the components, friction coefficient could not be measured directly as would ordinarily be desirable (as in the pin-on-disk configuration). We looked at friction coefficients that would be appropriate for this polymer/metal contact and then calculated the friction torques, which could then be compared with the experimentally measured values. We estimate the variation in the observed friction coefficient to be approximately 25 percent.

No leakage of water was observed through the contact. However, it was not possible with our test apparatus to verify that water never entered the contact since we were unable to probe the contact region.

Further experiments with a different torque sensor arrangement would be worthwhile, and we are in the process of redesigning the apparatus to give a wider range of information on friction torques. The major design tradeoff occurs between low-end sensor sensitivity and high-end sensor capacity, and our plan is to facilitate the ability to observe more of the high-end (failure) torque regime in future tests.